

## Impact of Si Oxidation States on Dipole Layer at HfO<sub>2</sub>/Si Interface

Noriyuki Miyata,<sup>1,2</sup> Yasuhiro Abe,<sup>2</sup> and Tetsuji Yasuda<sup>1</sup>

<sup>1</sup>National Institute of Advanced Industrial Science and Technology (AIST), Tsukuba, Ibaraki 305-8568, Japan

Phone: +81-29-861-2511, Fax: +81-29-861-5419, E-mail: nori.miyata@aist.go.jp

<sup>2,\*</sup>Musashi Institute of Technology, Setagaya-ku, Tokyo 158-8557, Japan

### 1. Introduction

Controlling interface Si oxide in the HfO<sub>2</sub> high-*k* gate-stack structure is one of the key issues in the development of advanced CMOS devices. Although the so-called direct-contact HfO<sub>2</sub>/Si interface, whose Si oxide is about one monolayer or less, has an advantage in the EOT scaling, a large negative  $V_{fb}$  shift, which is likely due to an dipole layer at the HfO<sub>2</sub>/Si interface, has been pointed out [1]. Several mechanisms have been proposed for the dipole formation at the HfO<sub>2</sub>/Si interfaces, *e.g.*, interface states, oxygen vacancies, and chemical bonding polarization [2-5]. In the chemical bonding model, charge transfer across the interface Si-O bonds is likely the dominant cause of dipole formation [4,5], so we may expect that the dipole-layer strength depends on the Si oxidation states at the HfO<sub>2</sub>/Si interface. In this work, we examine the dependence of dipole layer at HfO<sub>2</sub>/Si interfaces on post-deposition annealing (PDA) conditions, as interface Si oxidation proceeds during the PDA [6].

### 2. Experimental

Three types of experiments using *C-V*, Kelvin probe (KP), and XPS measurements were performed as shown in the *process flow*. The HfO<sub>2</sub> films were deposited on hydrogen-terminated Si(001) surfaces by using an ultra-high vacuum electron beam evaporation system [1,6]. The PDA were performed at 400-600°C in  $2 \times 10^{-6}$  Torr O<sub>2</sub> pressure. For the *C-V* measurement, MIS capacitors were fabricated using Ir electrodes. For the KP measurement, part of the SiO<sub>2</sub> area on the Si substrate was maintained as a reference surface.

### 3. Results and Discussion

The *C-V* curves shown in Fig. 1 show that small negative shift takes place after the 500°C PDA, and then large positive shift (toward the ideal position) takes place after the further 600°C PDA. The  $V_{fb}$ -versus- $T_{HfO_2}$  plot shown in Fig. 2 suggests that strength of dipole layer at the HfO<sub>2</sub>/Si interface increases after the 500°C PDA, and then decreases after the 600°C PDA. The contact potential difference (CPD) data of KP measurement shown in Fig. 3 indicate that charge distribution in the HfO<sub>2</sub>/Si structure depends on the PDA conditions. Figure 4 reveals that the potential difference ( $|\delta V_{CPD}|$ ) increases once, and then decreases dramatically during the PDA. This tendency is similar to the behavior observed by *C-V* measurement show in Figs. 1 and 2. Figure 5 suggests that the transition from the initial to the maximum potential difference corresponds to an increase of

the dipole-layer strength, because the potentials for both conditions do not depend on the HfO<sub>2</sub> thickness. On the other hand, the minimum potentials, which estimated for the long PDA time conditions (>400 sec), obviously depend on the HfO<sub>2</sub> thickness, suggesting that fixed charges are created in the HfO<sub>2</sub> films and the dipoles are likely eliminated under these PDA conditions. We therefore speculated that the MIS capacitors prepared under the 600°C-PDA conditions also include fixed charges. The dotted curve in Fig. 2 shows a calculated example where fixed negative charges of  $7.6 \times 10^{19} \text{ cm}^{-3}$  in the HfO<sub>2</sub> films, positive charges of  $2.5 \times 10^{13} \text{ cm}^{-2}$  at the HfO<sub>2</sub>/Si interface, and interface dipole of 0 V were assumed. From the above *C-V* and KP results, we concluded that the dipoles at the HfO<sub>2</sub>/Si interface are created during the initial PDA period, and are then eliminated during the following PDA period.

The Si 2*p* photoelectron spectra shown in Fig. 6 exhibit that sub-monolayer Si oxide exists at the initial HfO<sub>2</sub>/Si interface, and thick SiO<sub>2</sub> layer (>1 nm) is formed after the 600°C-PDA. Figure 7 reveals that the Si oxidation at the HfO<sub>2</sub>/Si interface proceeds slowly during the initial period, and then dramatic oxidation took place after the incubation period of about 220 sec. It is reported that such transition in the oxidation manner reflects the HfO<sub>2</sub> crystallization, *i.e.*, defects that cause the dissociation of O<sub>2</sub> molecules are created due to the HfO<sub>2</sub> crystallization [6]. It is important that the major potential change in the KP data shown in Fig. 4 takes place within the initial stage of the interface Si oxidation, suggesting that the HfO<sub>2</sub> crystallization is not the dominant cause of the dipole creation and annihilation.

Figure 8 indicates that the largest dipole layer is formed, when about one monolayer Si oxide grows at the HfO<sub>2</sub>/Si interface (where one-monolayer Si oxide was assumed to be 0.15 nm). The following dipole annihilation proceeds until about two-monolayer Si oxide grows. On the other hand, one monolayer Si oxide does not have Si<sup>4+</sup> oxidation states, but two-monolayer Si oxide has Si<sup>4+</sup> oxidation states. This suggests that the interface dipoles are related to oxygen-bonding configuration around the topmost Si atoms as shown in Fig. 9. The oxygen termination of topmost Si bonds may be responsible for the interface dipoles, and the oxygen insertion into the back bonds of topmost Si atoms releases the dipoles.

### 4. Conclusion

We experimentally demonstrated that dipoles at the direct-contact HfO<sub>2</sub>/Si interfaces strongly depend on the oxygen-bonding configuration around the interface Si atoms.

The maximum dipole layer was formed when the topmost Si bonds are terminated by oxygen, and then it was reduced due to the oxidation of Si back bonds.

### References

- [1] Y. Abe *et al.*, Appl. Phys. Lett. **90**, 172906 (2007).
  - [2] C. Hobbs *et al.*, VLSI Tech. Dig., (2003), p.9.
  - [3] K. Shiraishi *et al.*, VLSI Tech Dig., (2004), p. 108.
  - [4] P. W. Peacock *et al.*, Phys. Rev. B **73**, 075328 (2006).
  - [5] A. Kawamoto *et al.*, J. Appl. Phys., **90**, 1333 (2001).
  - [6] N. Miyata, Appl. Phys. Lett. **89**, 102903 (2006).
- \*Tokyo City University from April 1st, 2009.

### Process flow

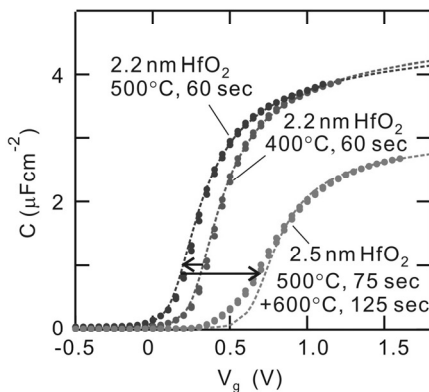
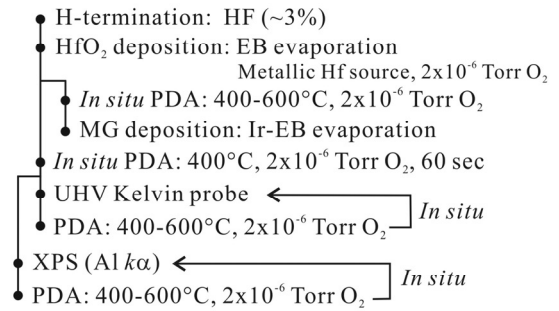


**Fig. 1** C-V curves of HfO<sub>2</sub>/Si structures prepared under various PDA conditions.

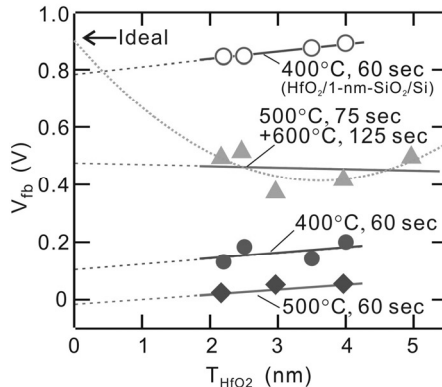


**Fig. 2** Dependence of  $V_{fb}$  for various PDA conditions on HfO<sub>2</sub> film thickness ( $T_{HfO_2}$ ).

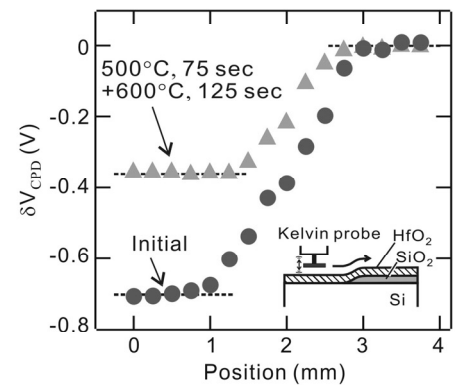


**Fig. 3** Effect of PDA on potential difference [ $\delta V_{cpd} = V_{cvd} - V_{cpd}$  (HfO<sub>2</sub>/SiO<sub>2</sub>/Si)].

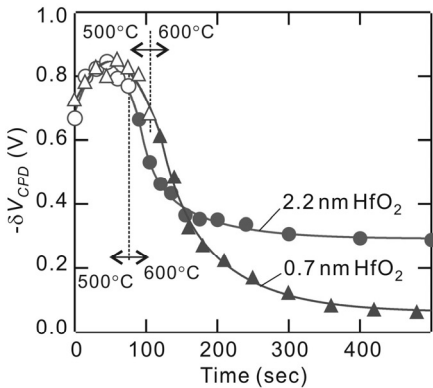


**Fig. 4** Dependence of potential difference ( $-\delta V_{cpd}$ ) on PDA time and HfO<sub>2</sub> film thickness.

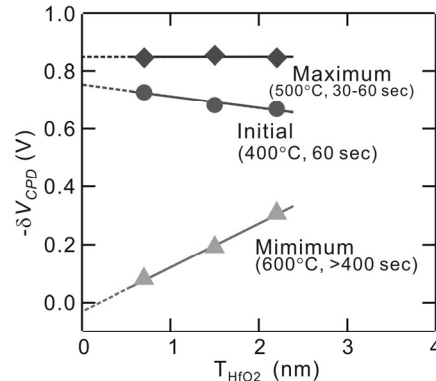


**Fig. 5** Dependence of initial, maximum, and minimum potential difference on HfO<sub>2</sub> film thickness ( $T_{HfO_2}$ ).

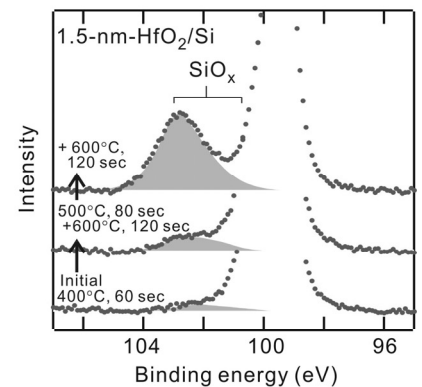


**Fig. 6** Si 2p photoelectron spectra of HfO<sub>2</sub>/Si structures prepared under various PDA conditions.

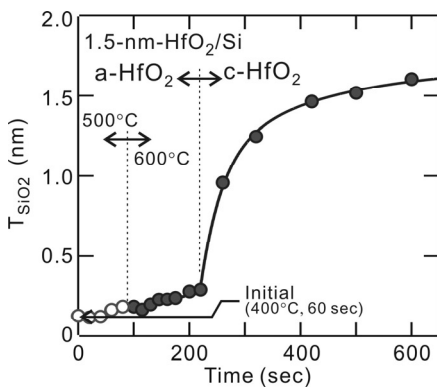


**Fig. 7** Si oxidation at HfO<sub>2</sub>/Si interface during PDA.

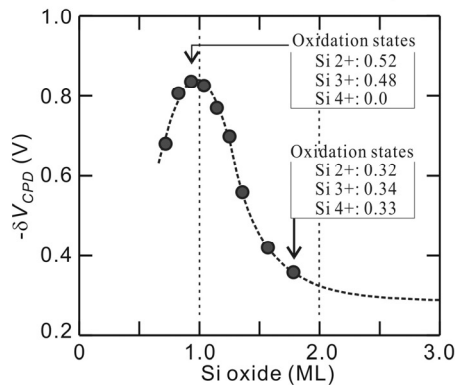


**Fig. 8** Potential difference versus interface Si oxide.

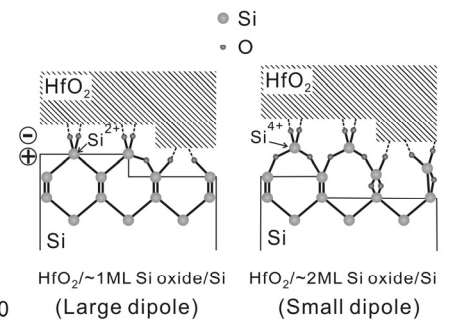


**Fig. 9** HfO<sub>2</sub>/Si interfaces with about 1 ML and 2 ML Si oxides